Otology & Neurotology
34:e76–e81 © 2013, Otology & Neurotology, Inc.

Cochlear Implantation Feasibility in Rhesus Macaque Monkey: Anatomic and Radiologic Results

*†Mathieu Marx, †‡§Pascal Girard, *||Bernard Escudé, †‡Pascal Barone, *Bernard Fraysse, and *†Olivier Deguine

**Department of Otology-Neurotology and Skull Base Surgery, Purpan University Hospital; †Centre National de la Recherche Scientifique, and ‡Université de Toulouse, UPS, Centre de Recherche Cerveau et Cognition; §Institut National de la Santé et de la Recherche Médicale; and ||Department of Neuroradiology, Clinique Pasteur, Toulouse, France*

Background: Large animal models of implantable hearing devices are needed to assess innovative technologies before using them in humans. The rhesus macaque has cognitive abilities close to humans and has been used in the past but with noncommercial implants or no detailed radiologic descriptions of the surgical procedures. The aim of this study was to evaluate the feasibility of cochlear implantation in this animal model.
Methods: We present detailed radiologic data (CT scan and Cone beam computed tomography) from 7 heads of rhesus macaque monkeys coming from autopsy materials. Several comparative measurements were performed with 10 human temporal bones to emphasize similarities and differences between the macaque and the human inner ear. The radiologic analyses helped planning the surgical approach for cochlear implant insertion in the macaque.
Results: We managed to perform one full (720 degrees) and 3 partial insertions (190–330 degrees) of cochlear implants in 4 rhesus macaque cochleae, documented by cone beam computed tomography reconstructions. We confirm that the procedure is facilitated in this animal because the cochlea dimensions are close to humans. However, marked differences in the orientation of the external auditory canal and the basal turn must be taken into account. We suggest that the removal of the inferior wall of tympanal bone provides the optimal axis for electrode array insertion.
Conclusion: The rhesus macaque monkey is a valid and close-to-human animal model for cochlear implants insertion. Because this species is widely used in both behavioral and physiologic studies, we expect that functional implants can be coupled with electrophysiologic recordings to study the mechanisms of auditory compensation. **Key Words:** Animal model—Cochlear implant—Cochlea size—Temporal bone anatomy.
Otol Neurotol **34:**e76–e81, 2013.

The use of cochlear implants as a neuroprosthetic substitute for hearing is growing worldwide. Because invasive studies are impossible on humans, animal models such as cats are required to improve technical issues or to understand the mechanisms of brain plasticity underlying restored audition (1). However, to the best of our knowledge, large animal models with cochlear implants of the type used in humans are only successfully represented by sheep (2). Because of phylogenetic proximity, a nonhuman primate model is the most comparable with humans and allows one to combine electrophysiologic studies with sophisticated perception behavior. In particular, rhesus macaque monkeys have complex cognitive capacities and, for instance, can be subjects of psychophysical investigations of visuo-auditory integration of face and voice (3), a major issue for implanted patients (4). Furthermore, such monkeys are used routinely as subjects of various studies on brain mechanisms that underlie high-order auditory processing (5).

A recent study successfully developed cochlear implants in the common marmoset monkey (6). They managed to insert a 5.7-mm-long cochlear implant (Hybrid-S H12; Cochlear, Sydney, Australia) in the marmoset through a cochleostomy. The small dimensions of the cochlea in the marmoset preclude the use of longer implants. However, studies with modern commercial implants in macaque monkeys are still lacking. Most previous studies on monkeys have only used noncommercial electrodes or much older models (7–10) or have not been developed for more than 15 years (11–14) but established that electrical devices could be permanently implanted and used in psychophysical tasks by the animals.

The present work aims at describing the surgical approach of cochlear implant in rhesus macaque monkeys (*Macaca Mulatta*). The description of the middle and inner

Address correspondence and reprint requests to Mathieu Marx, M.D., Department of Otology-Neurotology and Skull Base Surgery, Purpan University Hospital, Place du Docteur Baylac, 31059 Toulouse, France; E-mail: marx.m@chu-toulouse.fr
Mathieu Marx and Pascal Girard contributed equally to this work.
The authors disclose no conflicts of interest.

ear structures of the rhesus macaque from detailed dissection and histologic studies can be found in the work of Wysocki (15,16). They show that temporal bone anatomy and cochlea dimensions are close to what is observed in humans, which enhances the validity of this model.

The painstaking methodology used in these studies can be advantageously replaced by modern CT scan or cone beam CT imaging that allows precise measurements of the structures with the implant in situ. Such an approach has been performed in the marmoset (6) but not yet in the macaque monkey. The present study aims at providing detailed high-resolution radiologic imaging of the temporal bone structures and associated measurements of the cochlea in the rhesus macaque monkey. Imaging with cochlear implants in situ leads to the conclusion that a full insertion of the implant is feasible in the macaque monkey.

MATERIALS AND METHODS

Study Design

Seven frozen fresh heads of rhesus macaque monkey (*Macaca Mulatta*) were obtained from autopsy material provided by the SILABE platform. The autopsies did not require the use of formaldehyde fixation or equivalent. The individuals were normal adult male subjects ranging from 9 to 11 years old and weighting between 9.3 and 13.4 kg. In 4 specimens, we performed a unilateral cochlear implantation using a MedEl medium electrode array (24 mm; MedEl, Innsbruck, Austria). All specimens underwent a multislice helical CT scan and a cone beam CT. The scanner was a Philips helicoid 40-channel device. The high-resolution protocol used 2 channels in 0.5-mm collimation. We implemented every 0.55 mm with 0.1 mm increment.

The system used was a vertical NewTom VGI (NewTom, Verona, Italy). We immobilized the monkeys' heads with polystyrene plaques, and we implemented a high-resolution protocol. The system used a 200 × 25–mm flat panel detector at 650 mm from the radiation source. The 360-degree rotation of the X-ray tube took 18 seconds. Tube voltage was 110 kV, with a 19 mA charge at the terminals. Total filtration was 2 mm and pitch 125 μ, with field of view corresponding to a 12*7.5 cm diameter cylinder. Acquisition began with frontal and lateral of the temporal bone location of interest and lasted 18 seconds. We reconstructed the images in 125μ isometric voxels and obtained in axial, coronal, and sagittal planes.

Morphometric Study

In the nonimplanted temporal bones, we analyzed several criteria to describe a reliable surgical technique for cochlear implantation.

We performed first several measurements to describe the dimensions of the cochlea:

- Number of turns of the cochlea
- Cochlea size using CT scan sagittal oblique minimum intensity projection reconstructions which allowed us to determine two main diameters of the cochlea, distance A and B, as described in Escudé's study (17).
- Length of the basal turn determined as the line between the round window and the lateral wall of the cochlea in contact with medial wall, which reflects the coiling pattern of the basal turn (Fig. 1A).
- Diameter of the basal turn calculating its greatest diameters (superoinferior and lateromedial) on coronal oblique reconstructions of the cochlea through the modiolus (Fig. 1, B and C)
- Round window largest diameter from the ponticulus to the crista fenestra

Then, we assessed the global configuration and orientation of the cochlea with respect to other structures of the cranial base.

- Angle between the external auditory canal and the basal turn axis in coronal oblique and axial planes (Fig. 2, A and B). In the coronal oblique plane, the basal turn axis was defined as the line between in the inferior ridge of the round window and the medial wall of the cochlea. In the axial plane, the basal turn axis followed the initial portion of the spiral canal.
- Angle between the axis of the basal turn and a sagittal midline in the axial plane, as described in Martinez-Monedero et al. (18).

We also assessed these criteria in 10 human temporal bones, provided by the anatomy laboratory of the faculty, to highlight the hypothetical specificities in surgery for macaque monkey. The human bones were free of any otologic pathology.

In the four implanted macaque temporal bones, the insertion depth angle from the round window, the length of the inserted electrode array and the number of implanted electrodes were determined using coronal oblique minimum intensity projection. When possible, the location of the electrode array inside the cochlea was determined (scala tympani or scala vestibuli) using midmodiolar views and reconstructions perpendicular to the ascending part of the basal turn. These reconstructions have

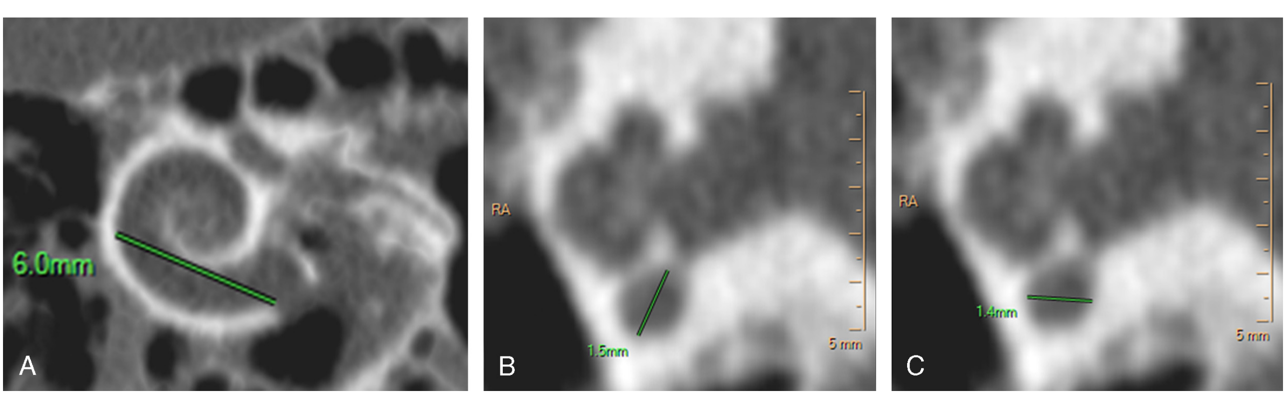

FIG. 1. *A*, Length of the basal turn in the left temporal bone of Monkey 4. *B*, Greatest superoinferior diameter of the basal turn on midmodiolar view in Monkey 5. *C*, Greatest lateromedial diameter of the basal turn on midmodiolar view in Monkey 5.

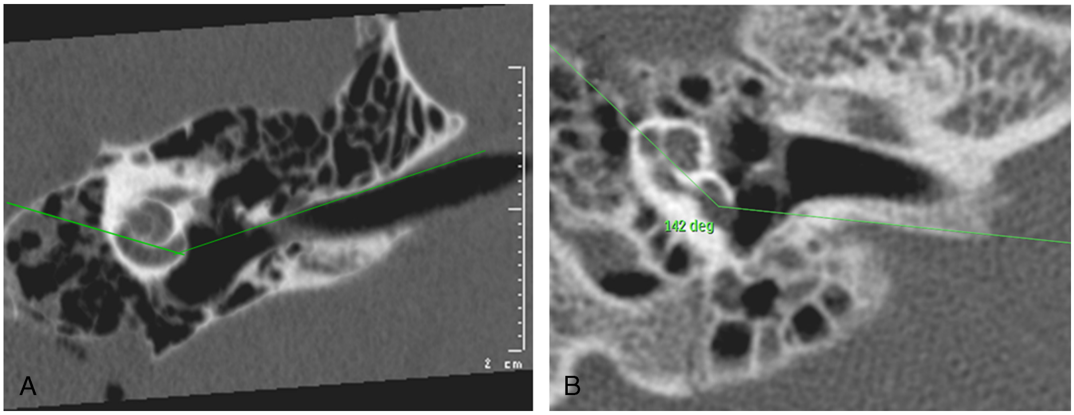

FIG. 2. Angles between the axis of the external auditory canal and the axis of the basal turn in coronal oblique plane (*A*) and axial plane (*B*) in Monkey 2.

been validated as a reliable tool to assess the electrode array position inside the human basal turn (19).

Surgical Procedure

The head was immobilized under a surgical microscope. We proceeded to a retroauricular opening to expose the mastoid bone and to raise a tympanomeatal flap from behind. We drilled the posterior and inferior wall of tympanal bone down to the digastric muscle. The third portion of the facial nerve was identified and preserved. This approach differs from the standard transfacial recess procedure used in humans and was chosen after CT scan analysis of the first nonimplanted heads. The upward orientation of the basal turn would have limited the insertion of the electrode array through a conventional posterior tympanotomy. The round window niche was then exposed and prepared as in humans, drilling the bony overhangs that surround the round window membrane itself. Finally, the electrode was inserted upward in the axis of the basal turn.

RESULTS

Anatomic Measurements

We obtained measurements in the non implanted temporal bone for 4 monkeys (M1 to M4) and measurements in both temporal bones for the remaining 3 monkeys (M5 to M7).

Figure 3, A and B, shows the minimum projection reconstruction obtained for the right cochlea in human 4 and the left cochlea of monkey 6. The procedure was identical to that used by Escudé and collaborators (17). It allows, on a 2D reconstruction plane of the basal turn, to compute the largest distance (A) between the round window and the lateral wall of the cochlea and its longest perpendicular distance (B).

The detailed of scanner measurements for both monkeys and humans temporal bones are reported in Table 1. In monkeys, all cochleae had 2.5 turns, which is also the mean value we measured for the humans. For each monkey, the difference between left and right ear in computation of distances A and B did not exceed .3 mm, hence was in the resolution range of the scanner. The mean values of A (6.34 mm, range: 5.8–6.8 mm) and B (4.76 mm; range: 4.2–5.3 mm) were respectively smaller than both mean values in humans (A: 8.95 mm, range: 8.3–9.7 mm; B: 6.84 mm, range: 6.3–7.6 mm). However, the ratio A/B was very similar (monkey: 1.33, Human: 1.31). Similarly, the length of the basal turn was always

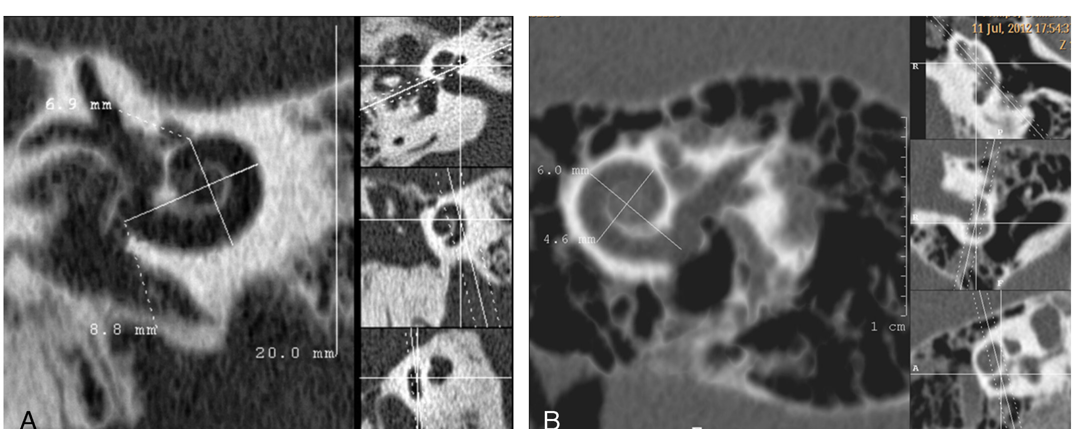

FIG. 3. Minimum intensity reconstructions and measurements of cochlea size obtained in Human 4 (*A*) and Monkey 6 (*B*).

TABLE 1. *Anatomic measurements in rhesus monkey and comparisons with human temporal bone*

	Monkey 1		Monkey 2		Monkey 3		Monkey 4		Monkey 5		Monkey 6		Monkey 7		Monkey (mean)	Human (mean)
	Right	Left	Right	Left	Right	Left	Right	Left	Right	Left	Right	Left	Right	Left		
No. of turns of the cochlea	2.5			2.5	2.5			2.5	2.5	2.5	2.5	2.5	2.5	2.5	2.5	2.5
Distance A (mm)	5.8			6	6			6.7	6.8	6.7	6.1	6	6.8	6.5	6.34	8.95
Distance B (mm)	4.2			4.6	4.6			4.7	4.8	4.9	4.8	4.6	5.1	5.3	4.76	6.84
Length of basal turn (mm)	5			5.3	5			6	5.7	5.6	5.1	5.3	5.9	5.6	5.45	8
Diameter of the round window (mm)	1.3			1.2	1.2			1.4	1.2	1.3	1.4	1.4	1.6	1.5	1.35	1.75
Diameter of the basal turn (superoinferior)	1.4			1.6	1.5			1.8	1.7	1.6	1.6	1.6	1.7	1.7	1.62	2.35
Diameter of the basal turn (latromedial)	1.1			1.4	1.4			1.4	1.5	1.5	1.4	1.5	1.4	1.4	1.4	1.97
Orientation of the basal turn (degrees)	43.2°			43.1	44.7			47.5	43.6	44.3	40.2	39.9	47.9	48.2	44.3	51.8
Angle between EAC and basal turn (axial plane) (degrees)	136			142	139°			152	149	147	143	147	157	150	146.2	142.8
Angle between EAC and basal turn (coronal reconstruction) (degrees)	167			164	167			152	149	162	151	153	160	164	159	194

reduced in monkeys (mean: 5.45 mm, range: 5–6 mm) compared with humans (mean: 8 mm, range: 7.7–8.3 mm). The coronal oblique diameters of the basal turn were also smaller in monkeys than in humans (respective mean values: 1.62 vs 2.35 mm for the superoinferior diameter and 1.4 vs 1.97 mm for the lateromedial diameter).

We measured the round window largest diameter from the ponticulus to the crista fenestra. The mean value for macaque monkey is 1.35 mm (range 1.2–1.6 mm; Table 1). Although it is smaller than the mean human value (1.75 mm), it is compatible with the electrode array dimensions (diameter of 0.5 mm at the apex and 0.8 mm in the basal portion).

The axial orientation of the basal turn with respect to the sagittal midline was slightly different between monkeys (mean value, 44.3 degrees; range, 39.9–47.5 degrees) and humans (mean value, 51.8; range, 49–55.8 degrees).

The anatomic comparison of macaque and human temporal bone revealed differences in the angle between

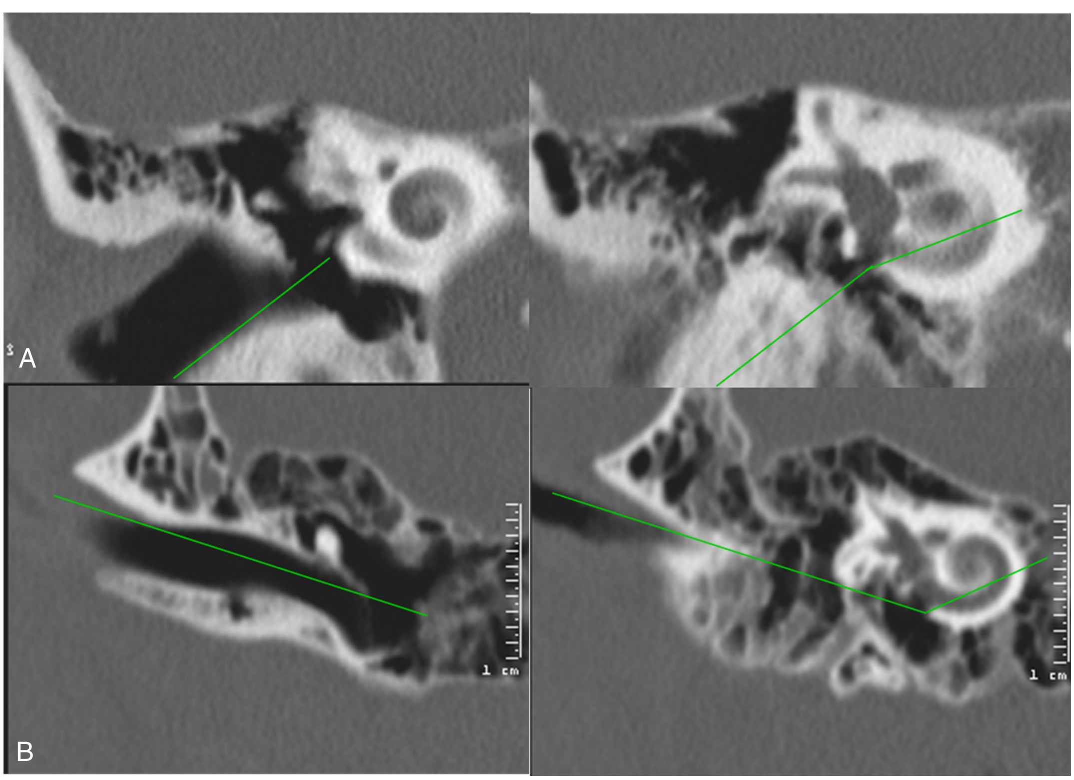

FIG. 4. Angle between EAC and the basal turn of the cochlea in the coronal oblique plane measured in Human 4 (*A*) and Monkey 5 (*B*). EAC axis is first determined (left) and then projected on a coronal slice including round window and the basal turn (right) to calculate the angle between the 2 axes.

TABLE 2. *Cochlear Implant measurements*

	Monkey 1	Monkey 2	Monkey 3	Monkey 4
Insertion depth angle	190°	720°	330°	240°
Length of electrode array inserted	9 mm	27 mm	12 mm	10 mm
No. of inserted electrodes (/12)	6	12	9	7

the external auditory canal (EAC) and the basal turn in both species (Table 1). The difference was particularly marked in coronal plane reconstructions (mean respective values for macaque and human: 159 and 194 degrees), whereas it was more modest in the axial plane (146.2 and 142.8 degrees). Therefore, the orientation of the EAC canal compared with the axis of the basal turn is obviously different between macaques and humans, as shown in Figure 4 coronal oblique reconstructions. In humans, EAC is directed upward and basal turn is horizontal in its initial part. In contrast, in the macaque the EAC and the basal turn of the cochlea present opposite orientations (respectively downward and upward). We had to take this difference into account to plan our surgical procedure. Hence, the surgical approach consisted in drilling the inferior and posterior wall of the tympanal bone to allow an insertion of the electrode array in a vertical axis (inferior to superior) rather than in the horizontal axis (posterior to anterior) classically used in humans.

Four electrode arrays were inserted in 4 different ears (Monkeys 1–4). Table 2 shows the measurements extracted from these insertions. The insertion depth angle was calculated on sagittal oblique minimum intensity projection reconstructions and was highly variable across macaque's temporal bones. Three implants were partially inserted but the insertion covered at least 180 degrees of the cochlea and involved at least half of the electrodes. One case (Monkey 2) consisted in a full insertion that is visible in cone beam sagittal oblique reconstruction (Fig. 5). The length of insertion was 27 mm, including the whole electrode array (24 mm) plus a more basal portion. Coronal oblique midmodiolar views and reconstructions perpendicular to the ascending part of the basal turn showed a scala tympani placement of the electrode array in the three partial insertions (M1, M3, and M4). The artifact surrounding the array did not allow us to determine its position in the specimen with full insertion (M2).

DISCUSSION

Our study shows, in specimen heads, that modern cochlear implants can be inserted successfully in the cochlea of the rhesus macaque monkey.

As in humans, morphologic reconstructions of the cochlea can be obtained in the rhesus macaque monkey by imaging with multislice helical CT scan and cone beam CT, the latter technique having a qualitatively better resolution and delivers less radiations than conventional CT scans (20). Indeed, although slightly smaller than in humans (17), the cochlea in macaque has a comparable number of turns and its dimensions are compatible with the dimensions of the implant. Interindividual variations are known in humans and cochlear dimensions of the rhesus are in the range seen with humans. In our study, mean round window diameter (1.35 mm) in macaque was also a little smaller than in humans, but it allowed the insertion of all current commercial electrode arrays. Our radiologic measurements were congruent with anatomical evidence provided by Wysocki (16), who found comparable mean length (1.31 mm) and height (1.29 mm). Similarities between human and macaque cochleae are counterbalanced by a major anatomical difference, which had to be taken into account before surgical procedure.

Because monkeys are not, as humans, highly specialized in bipedal locomotion, the orientation of the head with respect to the foramen magnum differs between humans and other primates (21–23). Indeed, we observed morphologic differences such that the angle of the skull base is tilted in monkeys. In contrast to humans, the

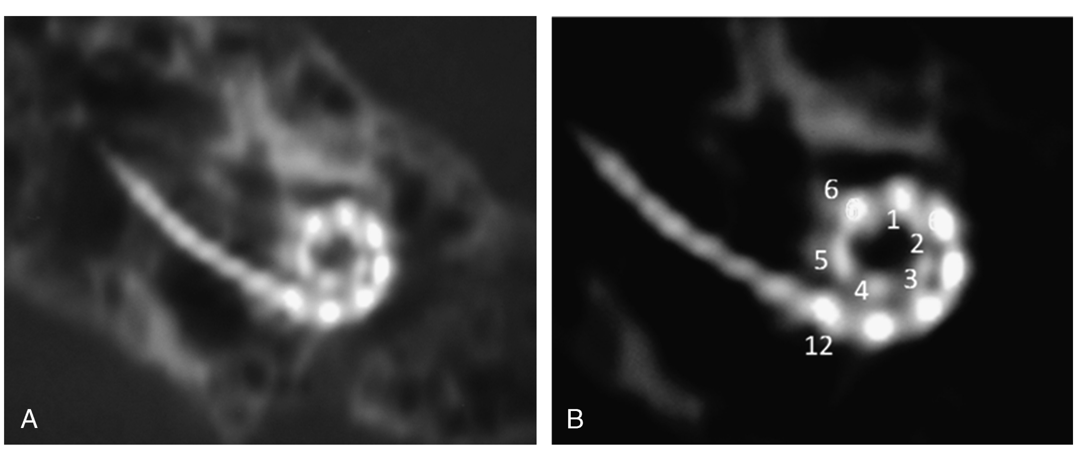

FIG. 5. Cone beam computed tomography reconstructions showing full insertion of the electrode array in Monkey 2 (*A*) with a zoom view on numbered electrodes (*B*).

petrous pyramid and external auditory canal are orientated downward, and the basal turn is upward. The angle we measured in temporal bones between EAC and basal turn axis was thus obviously smaller in macaque than in human. The specific upward orientation of basal turn in macaques made us discard the conventional posterior surgical approach through facial recess. We opted for a complete removal of inferior wall of tympanal bone and a partial drilling of its posterior part to enhance the insertion axis. This procedure, associated with middle ear exclusion, should not alter postsurgical recovery in animals.

Using this surgical procedure, we managed to perform three partial insertions, the feasibility of which is already mentioned in the literature (12). Those authors reported histologic analysis of 10 implanted temporal bones in macaque and found partial insertions in most of them (8 over 10) with seven insertions below 15 mm cochlear length. In this study, a full insertion was probably hard to achieve because the insertion axis was unfavorable. In our series, partial insertion might be related to the surgical installation. Indeed, a very declive position of the head is required to expose optimally the basal turn and may have been insufficient in the three specimens with partial insertion. A more rigid electrode array, eventually using a stylet, might also help covering more cochlear length. Finally, the variability in insertion depths might be related to an anatomic factor such as the diameter of the scala tympani in rhesus monkey cochlea. The study conducted by Wysocki and colleagues (16) provides such measurements, from the base to the end of scala tympani in Macaca rhesus. As in humans, the scala tympani dimensions decrease progressively and a height of 0.5 mm, that is the diameter of the tip of the electrode array used in our experiment, may be observed from 13 mm of cochlear depth, whereas such value is obtained beyond 25 mm in humans (24). This decrease in height of the scala tympani might account for our partial insertions and thinner electrode arrays, with a distal tip of 0.3 mm, might thereby be preferred in future experiments.

However, we achieved a full implantation at 720 degrees corresponding to 2 and a half turns and a length of the electrode array of 27 mm. This length corresponds to the mean length of the spiral canal in the rhesus macaque (15,16). The cochlea of this monkey did not have anomalous large dimensions that could explain the full insertion (Table 1). This full insertion was plausibly achieved at the price of a rupture of the basilar membrane between the scala tympani and the scala vestibuli in the middle turn.

We conclude that the rhesus macaque monkey with a cochlear implant is a valid model that can be revived in parallel with other interesting recent models such as the cat (25), marmoset (6), or the sheep (2). Numerous studies have clearly established this species as an essential model for neurophysiologic investigations in conjunction with sophisticated behavior. We think that adding the feasibility of cochlear implants in the macaque monkey opens a promising field of research on the issue of the mechanisms of auditory recovery after cochlear implant surgery.

REFERENCES

1. Kral A, Sharma A. Developmental neuroplasticity after cochlear implantation. *Trends Neurosci* 2012;35:111–22.
2. Schnabl J, Glueckert R, Feuchtner G, et al. Sheep as a large animal model for middle and inner ear implantable hearing devices: a feasibility study in cadavers. *Otol Neurotol* 2012;33:481–9.
3. Chandrasekaran C, Lemus L, Trubanova A, et al. Monkeys and humans share a common computation for face/voice integration. *PLoS Comput Biol* 2011;7:e1002165.
4. Rouger J, Lagleyre S, Demonet JF, et al. Evolution of crossmodal reorganization of the voice area in cochlear-implanted deaf patients. *Hum Brain Mapp* 2012;33:1929–40.
5. Rauschecker JP, Scott SK. Maps and streams in the auditory cortex: nonhuman primates illuminate human speech processing. *Nat Neurosci* 2009;12:718–24.
6. Johnson LA, Della Santina CC, Wang X. Temporal bone characterization and cochlear implant feasibility in the common marmoset (Callithrix jacchus). *Hear Res* 2012;290:37–44.
7. Balkany TJ, Mischke RE, Pauley JD, et al. Implanted cochlear prosthesis analogue in primates. *Otolaryngol Head Neck Surg* 1980;88:477–85.
8. Burnett PA, Miller JM, Mangham CA. Intra-aural reflexes elicited by a cochlear prosthesis in monkeys. *Hearing research* 1984;16:175–80.
9. Morris DJ, Pfingst BE. Effects of electrode configuration and stimulus level on rate and level discrimination with cochlear implants. *J Assoc Res Otolaryngol* 2000;1:211–23.
10. Pfingst BE, Donaldson JA, Miller JM, et al. Psychophysical evaluation of cochlear prostheses in a monkey model. *Ann Otol Rhinol Laryngol* 1979;88:613–25.
11. Burton MJ, Shepherd RK, Clark GM. Cochlear histopathologic characteristics following long-term implantation. Safety studies in the young monkey. *Arch Otolaryngol Head Neck Surg* 1996;122:1097–104.
12. Shepherd RK, Clark GM, Xu SA, et al. Cochlear pathology following reimplantation of a multichannel scala tympani electrode array in the macaque. *Am J Otol* 1995;16:186–99.
13. Burton MJ, Shepherd RK, Xu SA, et al. Cochlear implantation in young children: histological studies on head growth, leadwire design, and electrode fixation in the monkey model. *Laryngoscope* 1994;104:167–75.
14. Xu J, Shepherd RK, Xu SA, et al. Pediatric cochlear implantation. Radiologic observations of skull growth. *Arch Otolaryngol Head Neck Surg* 1993;119:525–34.
15. Wysocki J. Dimensions of the vestibular and tympanic scalae of the cochlea in selected mammals. *Hear Res* 2001;161:1–9.
16. Wysocki J. Topographical anatomy and morphometry of the temporal bone of the macaque. *Folia Morphol (Warsz)* 2009;68:13–22.
17. Escude B, James C, Deguine O, et al. The size of the cochlea and predictions of insertion depth angles for cochlear implant electrodes. *Audiol Neurootol* 2006;11:27–33.
18. Martinez-Monedero R, Niparko JK, Aygun N. Cochlear coiling pattern and orientation differences in cochlear implant candidates. *Otol Neurotol* 2011;32:1086–93.
19. Lecerf P, Bakhos D, Cottier JP, et al. Midmodiolar reconstruction as a valuable tool to determine the exact position of the cochlear implant electrode array. *Otol Neurotol* 2011;32:1075–81.
20. Dahmani-Causse M, Marx M, Deguine O, et al. Morphologic examination of the temporal bone by cone beam computed tomography: comparison with multislice helical computed tomography. *Eur Ann Otorhinolaryngol Head Neck Dis* 2011;128:230–5.
21. Daubenton LJ. Mémoire sur les differences de la situation du grand trou occipital dans l'homme et dans les animaux Histoire de l'Académie Royale des Sciences. Paris, 1764:568–79.
22. Spoor F, Zonneveld F. Comparative review of the human bony labyrinth. *Am J Phys Anthropol* 1998;41:211–51.
23. Lieberman DE, Ross CF, Ravosa MJ. The primate cranial base: ontogeny, function, and integration. *Am J Phys Anthropol* 2000;117–69.
24. Wysocki J. Dimensions of the human vestibular and tympanic scalae. *Hear Res* 1999;135:39–46.
25. Kral A, Hartmann R, Tillein J, et al. Hearing after congenital deafness: central auditory plasticity and sensory deprivation. *Cereb Cortex* 2002;12:797–807.